Acta Pharmaceutica Sinica B 2021;11(7):2059–2069

Chinese Pharmaceutical Association
Institute of Materia Medica, Chinese Academy of Medical Sciences

Acta Pharmaceutica Sinica B

www.elsevier.com/locate/apsb
www.sciencedirect.com

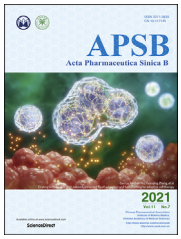

ORIGINAL ARTICLE

Molecularly engineered truncated tissue factor with therapeutic aptamers for tumor-targeted delivery and vascular infarction

Bozhao Li[a,b], Jingyan Wei[a,*], Chunzhi Di[b,c], Zefang Lu[b,c], Feilong Qi[b,c], Yinlong Zhang[b,c], Wei Sun Leong[d], Lele Li[b], Guangjun Nie[b,c,*], Suping Li[b,c,*]

[a]*College of Pharmaceutical Science, Jilin University, Changchun 130021, China*
[b]*CAS Key Laboratory for Biomedical Effects of Nanomaterials & Nanosafety, CAS Center for Excellence in Nanoscience, National Center for Nanoscience and Technology, Beijing 100190, China*
[c]*Center of Materials Science and Optoelectronics Engineering, University of Chinese Academy of Sciences, Beijing 100049, China*
[d]*Department of Materials Science and Engineering, National University of Singapore, 117575, Singapore*

Received 22 May 2020; received in revised form 21 July 2020; accepted 17 August 2020

KEY WORDS

Tumor targeted delivery;
Truncated tissue factor (tTF);
AS1411 aptamer;
Thrombosis;
Tumor infarction

Abstract Selective occlusion of tumor vasculature has proven to be an effective strategy for cancer therapy. Among vascular coagulation agents, the extracellular domain of coagulation-inducing protein tissue factor, truncated tissue factor (tTF), is the most widely used. Since the truncated protein exhibits no coagulation activity and is rapidly cleared in the circulation, free tTF cannot be used for cancer treatment on its own but must be combined with other moieties. We here developed a novel, tumor-specific tTF delivery system through coupling tTF with the DNA aptamer, AS1411, which selectively binds to nucleolin receptors overexpressing on the surface of tumor vascular endothelial cells and is specifically cytotoxic to target cells. Systemic administration of the tTF-AS1411 conjugates into tumor-bearing animals induced intravascular thrombosis solely in tumors, thus reducing tumor blood supply and inducing tumor necrosis without apparent side effects. This conjugate represents a uniquely attractive candidate for the clinical translation of vessel occlusion agent for cancer therapy.

© 2021 Chinese Pharmaceutical Association and Institute of Materia Medica, Chinese Academy of Medical Sciences. Production and hosting by Elsevier B.V. This is an open access article under the CC BY-NC-ND license (http://creativecommons.org/licenses/by-nc-nd/4.0/).

*Corresponding authors.
E-mail addresses: jingyanweijluedu@163.com (Jingyan Wei), niegj@nanoctr.cn (Guangjun Nie), lisuping@nanoctr.cn (Suping Li).
Peer review under responsibility of Chinese Pharmaceutical Association and Institute of Materia Medica, Chinese Academy of Medical Sciences.

https://doi.org/10.1016/j.apsb.2020.11.014
2211-3835 © 2021 Chinese Pharmaceutical Association and Institute of Materia Medica, Chinese Academy of Medical Sciences. Production and hosting by Elsevier B.V. This is an open access article under the CC BY-NC-ND license (http://creativecommons.org/licenses/by-nc-nd/4.0/).

1. Introduction

In order for tumors to grow, tumor blood vessels are required for the delivery of oxygen and nutrients, and the removal of metabolic waste products[1]. Thus, the selective thrombotic occlusion of tumor vessels, to starve tumors to death, is of particular interest in cancer therapy[2−4]. In contrast to the existing cancer therapeutics, which takes months or years of treatment to achieve remission, the therapeutic effects of tumor vessel occlusion typically occur within days, especially in cases of large, solid tumors, which are rich in blood vessels[5−7]. In addition, the issue of drug resistance, which is a critical challenge in cancer treatment, can be overcame by vascular occlusion. Thus far, truncated tissue factor (tTF)-based vascular coagulation agents are the most popular[8−11]. tTF is the extracellular domain of the coagulation inducing protein, tissue factor (TF), which is the initiator of the extrinsic coagulation pathway[12−14]. Although free tTF has an affinity for the binding site of FVII or FVIIa, as well as a capacity to activate FX and FIX, tTF has a limited ability to induce coagulation due to changes in the protein's conformation and lack of a transmembrane domain. It has been shown that the ability of tTF to activate FX is greatly reduced, compared to full-length tissue factor. Therefore, placing tTF in proximity to a phospholipid membrane is essential to recover its potent coagulation activity[15−20]. In consideration of this property, peptide ligands or antibodies that recognize different tumor endothelial markers have been fused to tTF to specifically deliver this protein to tumor vessels for tumor infarction[6−11]. Although a large number of tTF delivery strategies have proven to be effective in inducing intratumor thrombosis to incur tumor necrosis in animal models, most of these methods have not been translated to clinical use due to various drawbacks, such as low biosafety and poor tumor specificity[8,11]. The development of novel strategies to deliver tTF to tumor vessels with high tumor specificity and good tolerability are still needed to boost clinical practice of vascular occlusion agents.

AS1411 aptamer is a guanosine rich single stranded DNA oligonucleotide segment being able to selectively bind to nucleolin receptors, which are overexpressed on the surface of tumor cells and tumor vascular endothelial cells[21−25]. AS1411 also exhibits marked cell killing ability in response to binding to its receptor[26,27]. In contrast to antibodies or peptide ligands, DNA/RNA aptamers have several unique advantages: (1) specific, stable three-dimensional shape that confers a long *in vivo* half-life, and precise and tight binding to targets; (2) therapeutic activity with low immunogenicity; (3) small size and high structure stability, making them easily and cost-effectively synthesized[28−30]. A number of different studies therefore have used aptamers as efficient delivering vehicles to specifically deliver cytotoxic agents to tumor sites for effective therapy[31−34]. Our group recently developed a self-assembled DNA nanorobot functionalized with AS1411 aptamers on its external surface to realize the precise delivery of coagulation induction protease, thrombin, solely to tumor sites for safe and effective tumor therapy[33].

Inspired by these findings, we herein report a novel structure of tTF-AS1411 conjugate, wherein tTF protein was coupled with AS1411 aptamer in a few steps with high yield and purity. Using tumor-bearing animal models of liver cancer and melanoma, we demonstrate that intravenously administered tTF-AS1411 specifically bound to the tumor-associated vessels and induced intravascular thrombosis, shutting off tumor blood supply and inducing tumor necrosis. This easily synthesized conjugate with reliable property and low cost provides possibility for moving therapeutic vessel occluding agent into clinical application.

2. Material and methods

2.1. Preparation of tTF protein

The tTF and tTF-pHLIP (a control for tTF-AS1411) proteins were all synthesized *de novo*, similar to the methods described in our previous work[8]. In brief, the cDNA encoding tTF or tTF-pHLIP was cloned into the pET-30a(+) vector and vectors were then transfected into BL21DE3 cells, followed by stimulating with IPTG for 3 h. After that, the supernatants were collected and filtered through the 0.22 μm filter. The proteins were purified using the His Bind Kit (Merck Millipore, catalog No. 70239−3, Billerica, MA, USA) and dialyzed against Tris buffer to remove the salt.

2.2. tTF-AS1411 conjugation

AS1411 (5′-polyA-GGTGGTGGTGGTTGTGGTGGTGGTGG-3′) with a 5′-$(CH2)_{12}$-SH modification, was purchased from Sangon Biotech (Shanghai, China). For coupling AS1411 with tTF, a linker, sulfo-SMCC [sulfosuccinimidyl 4-(*N*-maleimidomethyl) cyclohexane-1-carboxylate (Abcam, catalog No. ab145607, Shanghai, China] was used. Sulfo-SMCC provides maleimide groups to react with the thiol from AS1411 and NHS ester to react with NH_2 in the C-terminus of tTF. Briefly, 2 μL 30 mmol/L TCEP (yuanye Bio-Technology Co., Ltd., catalog No. S16054, Shanghai, China) in deionized water and 2 μL 1 mol/L sodium phosphate buffer (pH 5.5) were added to 30 μL 1 mmol/L thiol-DNA in deionized water. The reaction was incubated at r.t. for 1 h and the products were then purified using an Amicon-3K (Merck Millipore, catalog No. UFC500324, Billerica, MA, USA) centrifugation filter concentrator with Buffer A (0.1 mol/L sodium phosphate buffer, 0.1 mol/L NaCl, pH 7.3) for 8 rounds of centrifugation. Next, 1 mg Sulfo-SMCC (Abcam) was added to 800 μL 1 mg/mL tTF in Buffer A, after which the solution was vortexed for 5 min and placed on a shaker for 2 h at r.t. The mixture solution was purified with an Amicon-3K (Merck Millipore) with Buffer A for eight rounds of centrifugation to remove the excessive Sulfo-SMCC. The activated tTF and the thiol-DNA solutions were mixed at r.t. for 36 h. To remove excess thiol-DNA, the mixture was centrifuged using an Amicon-30 K (Merck Millipore, catalog No. UFC503008, Billerica, MA, USA) with Buffer A for 8 times. To ensure the ratio of tTF protein and AS1411 per conjugate, the next purification was performed in an Amicon-50 K (Merck Millipore, catalog No. UFC505024, Billerica, MA, USA) with Buffer A for 8 rounds of centrifugation. The liquid flowed out after centrifugation was collected and concentrated with an Amicon-3K tube (Merck Millipore).

2.3. Synthesis of Cy5.5-labeled tTF or tTF-AS1411

For labeling of tTF, 100 nmol Cy5.5 NHS ester (Fanbo Biochemicals, catalog No. 1054, Beijing, China) was added into a tTF solution (10 nmol in 300 μL PBS, pH 8.0). The mixture was incubated at r.t. for 4 h with gentle shaking. The Cy5.5 labeled tTF was purified with an Amicon-3K (Merck Millipore) for three rounds of centrifugation. For the labeling of tTF-AS1411, AS1411 (5′-PolyA-GGTGGTGGTGGTTGTGGTGGTGGTGG-3′) pre-

conjugated with the Cy5.5 which has a 5′-$(CH2)_{12}$-SH and a 3′-Cy 5.5 modification were purchased from Sangon Biotech (Shanghai, China).

2.4. Characterization of tTF-AS1411 conjugate

To verify the successful formation of the tTF-AS1411conjugate, we subjected the products to SDS-PAGE and Western blot experiments. tTF and tTF-AS1411 protein were boiled for 10 min in SDS-PAGE loading buffer. The Electrophoresis System (Bio-Rad, Hercules, CA, USA) with a 10% polyacrylamide gel was used to resolve the different proteins. To visualize the result, the gel was incubated with Coomassie brilliant blue solution for 4 h and then destained overnight. Afterwards the gel was acquired by the Imaging System (Bio-Rad). For the Western blot experiment, tTF protein in the 10% polyacrylamide gel was electrophoretically transferred to a poly (vinylidene difluoride) membrane, which was then blocked with 5% non-fat milk in TBST (tris-buffered saline containing 0.02% Tween 20) for 1 h and incubated with a tTF antibody (Cloud-Clone Corp, catalog No. PAA524Hu01, Wuhan, Hubei, China) overnight at 4 °C. After having washed three times with TBST, the membranes were incubated with the IgG-HRP secondary antibody (Sangon Biotech, catalog No. C000939, Shanghai, China) for 1 h. The blot image was visualized by the Imaging System (Bio-Rad, Hercules, CA, USA).

2.5. Coagulation activity of tTF-AS1411 in vitro

To simulate the cellular membrane structure, the liposomes were prepared by mixing phosphatidylcholine (Solarbio, catalogNo. YZ-1535733, Beijing, China) and phosphatidylserine (Macklin, catalog. S832149, Shanghai, China.) at a volume ratio of 7:3. The mixture was then sonicated for 20 min and diluted with TBSA (TBS containing 0.1% bovine serum albumin, BSA, Amresco, Solon, OH, USA) to OD_{600} = 0.1.200 μL saline, tTF (40 μg) or tTF-AS1411 (40 μg) were mixed with 200 μL liposomes, respectively, and 200 μL 50 mmol/L $CaCl_2$ was then added and the samples immediately mixed in a 37 °C water bath for 1 h. The thrombin time was measured by the coagulation analyzer (LG-PABER-I, Taizhou, China).

2.6. Cell culture

MHCC-97H liver cancer cells, B16−F10 melanoma cells and human umbilical vein endothelial cells (HUVECs) were purchased from the National Platform of Experimental Cell Resources for Sci-Tech (Beijing, China). All cell lines maintained in a humidified incubator at 37 °C with 5% CO_2. The MHCC-97H and B16−F10 cells were cultured in DMEM media (WISENT, catalog No. 319-061-CL, Nanjing, China) supplemented with 10% FBS (WISENT, catalog No. 086−150, Nanjing, China), while the HUVECs were cultured in F12K medium (WISENT, catalog No. 312-250-CL, Nanjing, China) containing 10% FBS (WISENT) or F12K medium (WISENT) containing 10% FBS (WISENT) and vascular endothelial growth factor (VEGF, 100 ng/mL, Beyotime, catalog No. P5606, Shanghai, China).

2.7. Flow cytometry

5.0×10^4 HUVECs were suspended in phosphate buffer at pH 7.4 in the presence of tTF-Cy5.5, tTF-AS1411-Cy5.5 or tTF-AS1411-Cy5.5 (20 μg tTF for each formulation) and incubated with an anti-nucleolin antibody (1:1000, Abcam, catalog No. ab129200, Shanghai, China) for 30 min at 37 °C. The cells were washed three times with PBS and then resuspended in 600 μL PBS for flow cytometry analysis (Becton and Dickinson C6, Franklin Lake, NJ, USA).

2.8. Confocal microscopy

HUVECs were maintained in confocal microscopy dishes (2 cm diameter; 5.0×10^3/dish, Nunc, catalog No. 801002, Shanghai, China.) and cultured in F12K media (WISENT) supplemented with 10% FBS (WISENT) and 100 ng/mL VEGF (Beyotime). After 24 h, the media was discarded and cells were washed three times with phosphate buffer saline. Cy5.5-labeled tTF, Cy5.5-labeled AS1411 or Cy5.5-labeled tTF-AS1411 was then added to cells that were pretreated with anti-nucleolin antibody (Abcam) or not. After 30 min, the cells were washed three times with phosphate buffer saline. DiO (Solarbio, catalog No. D5840, Beijing, China) dye was used to stain the cell membranes and Hoechst 33342 (Solarbio, catalog No. B8040, Beijing, China) was used to stain cell nuclei. The FV1000-IX81 confocal microscope (Olympus, Tokyo, Japan) was used to acquire and analyze images.

2.9. Animal models

Six to eight-week-old BALB/c nude mice weighing 20 g were purchased from Beijing Vital River Laboratories and acclimated for at least ten days in our animal facility before experimentation. The mice were maintained at 50% humidity and 22 °C with the 12 h light to dark cycle. Human liver cancer MHCC-97H cells or mouse B16−F10 melanoma cells were dispersed in trypsin and resuspended with cold PBS. 50 μL single cell suspensions of MHCC-97H or B16−F10 tumor cell lines ($\sim 2 \times 10^6$ cells) mixed with 50 μL Matrigel (BD Pharmingen, catalog No. 354234, Franklin Lake, NJ, USA) were injected subcutaneously. In different time points, the tumor volume was evaluated by a vernier caliper, with the equation of length × $width^2/2$. In the process of long-term therapeutic, the tumor-bearing mice were injected with 100 μL saline, tTF (20 μg), AS1411 (0.75 nmol; synthesized by Sangon Biotech (Shanghai, China), tTF (20 μg) plus AS1411 (0.75 nmol), tTF-pHLIP or tTF-AS1411 (20 μg) every six days *via* a tail vein. The mice were euthanized under deep ketamine/xylazine anesthesia by cervical dislocation. Animal experiments were approved by the Committee on the Ethics of Animal Experiments of the Health Science Center of Peking University, Beijing, China.

2.10. Detection of intratumoral evans blue

The mice-bearing MHCC-97H tumors ($\sim$200 mm^3) were randomized into three groups and injected with tTF-AS1411 (20 μg), tTF (20 μg) or saline through a tail vein (n = 3). Twelve hours later, 5% Evans blue solution (100 μL, Macklin, catalog No. 314-13-6, Shanghai, China) was injected into the mice through a tail vein. Three hours later, the tumors were harvested, and the Evans blue dye was obtained by deal tumor tissues with tissue fixative solution for two days. The supernatants samples were detected by a UV−Vis spectrophotometer (AOE, A549, Shanghai, China) at the 620 nm wavelength to confirm the Evans blue content.

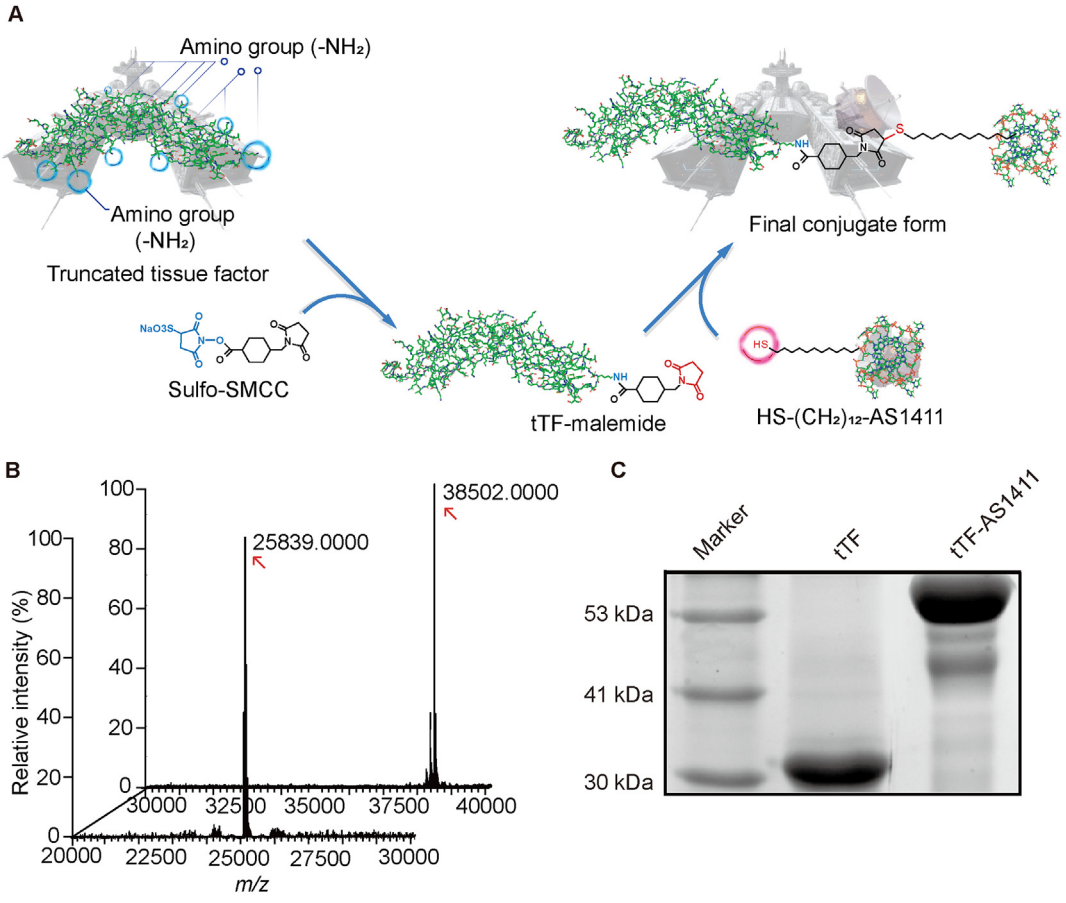

Figure 1 Synthesis and characterization of tTF-AS1411 conjugate. (A) Schematic diagram outlining the synthesis of tTF-AS1411. Sulfo-SMCC, which provides maleimide groups to react with the thiol (−SH) in AS1411 and NHS ester to react with the NH_2 in truncated tissue factor (tTF), was used as a linker. From a moral point of view, free tTF protein is a warship without radar, thereby being not able to precisely attack tumor tissues; however, linkage of AS1411 (as a radar) makes the warship selective for tumors. (B) The molecular weight of tTF and tTF-AS1411 were measured by HPLC−Q-TOF MS. (C) Gel electrophoretic migration of tTF and tTF-AS1411 verifies the conjugation of tTF to the aptamer, wherein tTF-AS1411exhibits a slower migration rate.

2.11. *In vivo imaging*

For investigating the *in vivo* biodistribution and tumor targeting of tTF-AS1411, 100 μL tTF-AS1411-Cy5.5 or tTF-Cy5.5 was intravenously administered into BALB/c nude mice with ∼200 mm^3 MHCC-97H liver tumors. At different time points, the mice were sacrificed and major organs and the tumors were removed and imaged with the 670 nm excitation and the 695 nm emission filter by the Maestro CRi imaging system (Waltham, MA, USA). To evaluate the blood perfusion of tumors, the mice with MHCC-97H liver tumors were injected 20 μg tTF-AS1411 or 100 μL 0.9% saline. After 10 h, 2 nmol AngioSense680 Ex, a blood pool contrast agent (PerkinElmer, catalog No. NEV10054EX, Waltham, MA, USA) were given to the mice. After another 24 h later, the fluorescence intensity in the tumors was detected using the 680 nm excitation and the 720 nm emission filter with a Maestro CRi imaging system (PerkinElmer, Waltham, MA, USA).

2.12. *Histological analysis*

For detecting thrombi, the BALB/c nude mice (n = 6, female) were injected weekly with tTF-AS1411 for four weeks (once per week). On week five, the tissues, including the heart, liver, spleen, lung and kidney were removed and fixed with 4% paraformaldehyde. The paraffin-embedded tissues were sectioned at 4 μm and transferred onto glass slides for H&E staining.

2.13. *ELISA assay*

Indirect ELISAs were used to assess the anti-tTF-AS1411 IgG titer. Briefly, plates (96 wells, Corning Costar, New York, NY, USA) were incubated with 10 μg/mL tTF-AS1411 in phosphate buffer saline for 4 h at room temperature then washed three times with PBST (0.1% Tween-20) and were blocked with PBS containing 1% BSA for further 2 h. BALB/c nude mice (n = 6, female) that non-tumor bearing were injected with tTF-AS1411 for 4 weeks (once per week). At week five, the serum was collected following centrifugation of whole blood collected from the mice. The serum of mice was diluted with a ratio from 1:10 to 1:1280. Next, 100 μL of the different dilution samples were cultured for 1 h at r.t. After rinsing the samples three times with PBST, a secondary antibody conjugated with HRP (goat-anti mouse IgG-HRP, Pierce, Rockford, IL, USA; 1:5000 in PBS with 1% BSA) was added to the samples for another 1 h. After washing three times with PBST, the TMB component (Merck-Millipore, Munich, Germany) was added to coloration, and then added HCl solution to end the

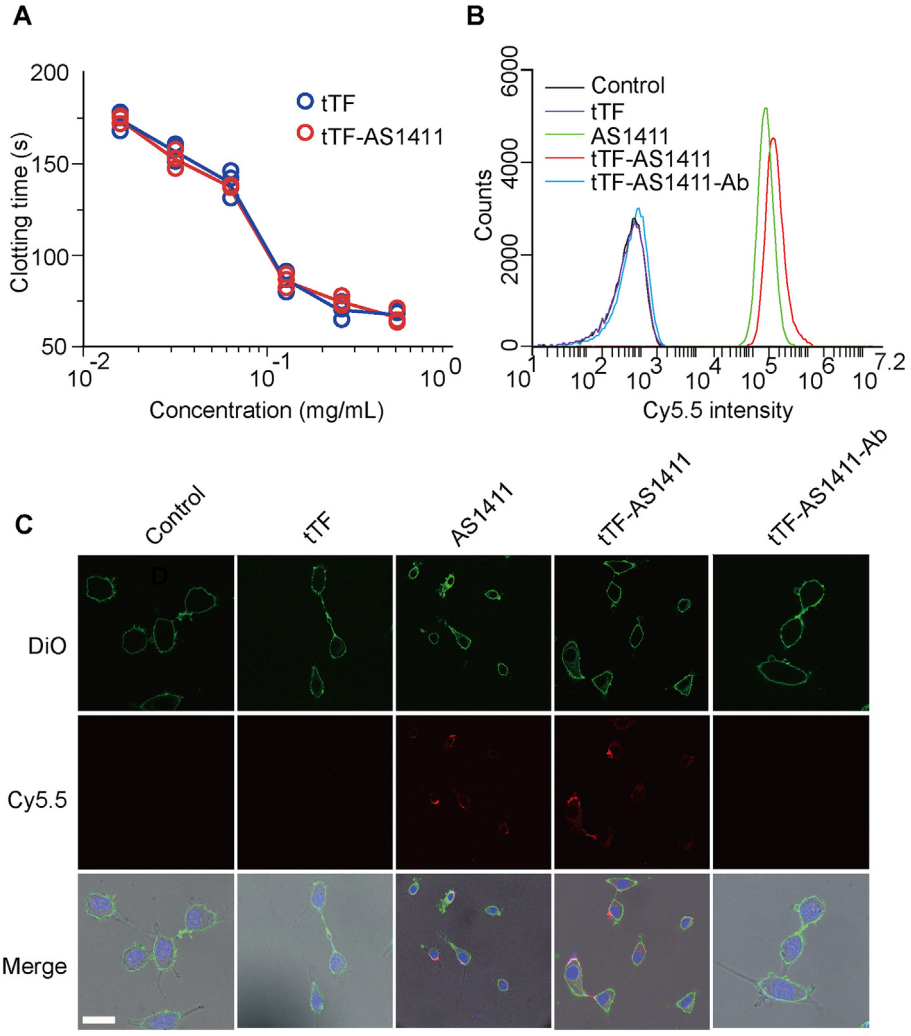

Figure 2 *In vitro* functional characterization of the conjugate. (A) Coagulation inducing activity of tTF and tTF-AS1411. (B) Targeting assessment of the Cy5.5-labeled tTF-AS1411 or various controls to V-HUVECs by flow cytometry analysis. (C) Representative confocal images of V-HUVECs after incubating with Cy5.5-labeled tTF-AS1411 (10 nmol/L) or controls for 30 min. Cell membranes and nuclei were stained with DiO (green) and Hoechst 33342 (blue), respectively. Scale bar = 20 μm.

reaction. The absorption intensity of 450 nm wavelength was assessed with a microplate (Biotek Instruments, Winooski, VT, USA).

2.14. *Statistical analysis*

Statistical differences between groups were assessed by *t*-test and among multiple groups was assessed by one-way ANOVA. Cumulative survival was compared using the Log-rank test. *P* values lower than 0.05 were considered statistically significant, $^{*}P < 0.05$, $^{**}P < 0.01$, $^{***}P < 0.001$.

3. Results

3.1. *Preparation and characterization of tTF-AS1411 conjugate*

The conjugation of tTF protein with AS1411 was achieved by a Sulfo-SMCC linker, which provides maleimide groups to react with the thiol from AS1411 and NHS ester to react with NH_2 in the tTF (Fig. 1A). For this conjugation, tTF proteins were first expressed by transfecting the pET-30a (+) expression vector containing DNA sequence encoding tTF into competent *Escherichia coli* cells. SDS-PAGE and HPLC-Q-TOF MS assay verified the expected molecular weight of tTF ~26 KD with a high purity (Fig. 1B, and Supporting Information Fig. S1). Sulfo-SMCC was then linked with the purified tTF in sodium phosphate buffer, followed by the addition of thiol-aptamer to form the final formulations *via* the Michael addition reaction between the thiol from DNA sequence and the maleimide in the Sulfo-SMCC. The successful linkage between tTF and AS1411 was verified by the fact that tTF-AS1411 had a larger molecular weight (~38 KD) than tTF alone (Fig. 1B) and a slower electrophoretic mobility (Fig. 1C). More importantly, it could be expected according to HPLC-Q-TOF MS data that the molecular ratio of tTF and AS1411 was 1:1 for each tTF-AS1411 conjugate.

3.2. *In vitro activity of tTF-AS1411*

To determine whether the addition of AS1411 aptamer will affect the coagulatory function of tTF protein, we assessed the blood coagulation-induced ability of tTF-AS1411 *in vitro*. Our

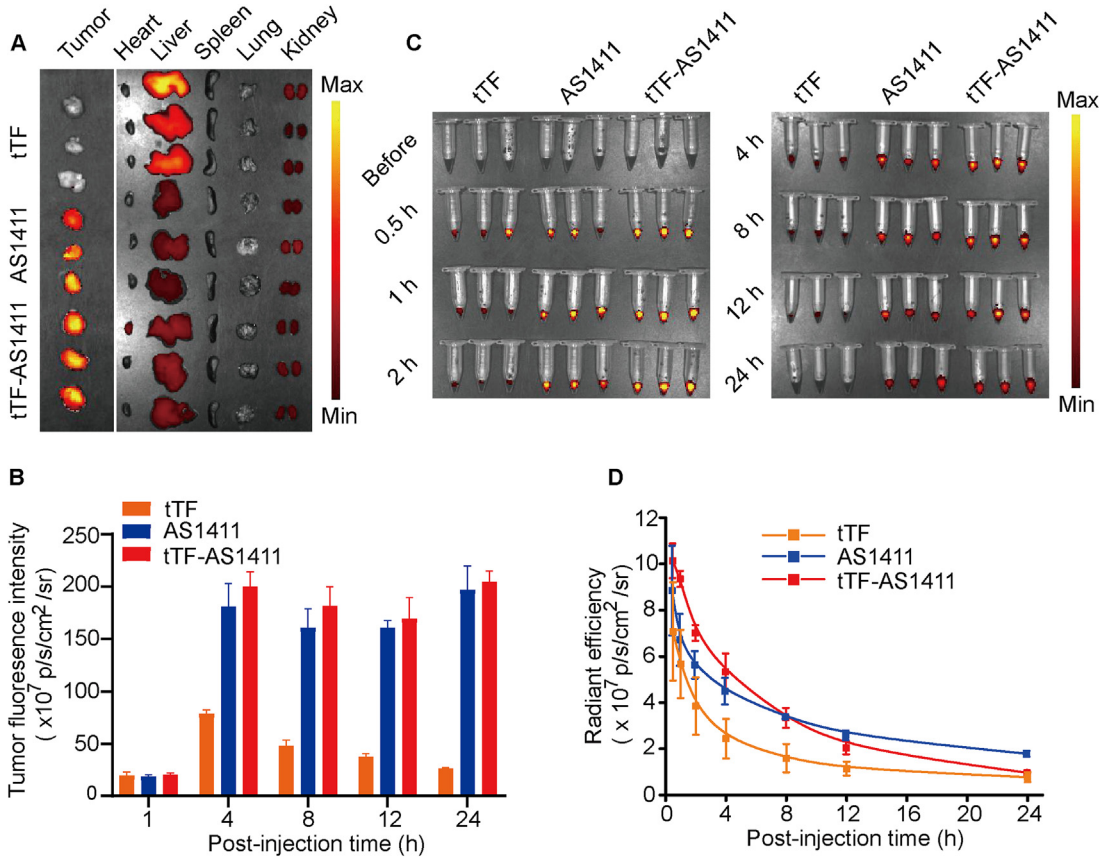

Figure 3 Tissue biodistribution and plasma pharmacokinetics. (A) Fluorescence images of tumors and organs removed from MHCC-97H liver tumor-bearing mice 24 h after injection of saline, tTF or tTF-AS1411 *via* the tail vein, $n = 3$ (B) Tumor fluorescence intensity after injection with various formulations as a function of time, n = 3. (C) Fluorescence images of the plasma samples collected from the mice at the indicated time points after administration of various formulations with a fluorescence imaging system. Error bars represent the mean ± SD, $n = 3$. (D) Plasma pharmacokinetic curves based on the quantified fluorescence intensities of the data of C. Error bars represent the mean ± SD, $n = 3$.

results showed that there was no significant difference in the blood clotting time after addition of either tTF-AS1411 or tTF alone into standard plasma at the same dosage (Fig. 2A), indicating that the coupling of the aptamer to tTF did not influence the protein's coagulation activity. We next evaluated the binding selectivity of tTF-AS1411 to tumor vascular endothelial cells using flow cytometry and confocal microscopy experiments. Human umbilical vein endothelial cells (HUVECs) cultured with addition of vascular endothelial growth factor (V-HUVECs) was commonly used *in vitro* as a representative malignant endothelial cell line with the high expression level of nucleolin on the cell membrane surface, and normally cultured HUVECs (N-HUVECs) is a nonmalignant cell line with almost no nucleolin expression on the membrane[35]. N-HUVECs and V-HUVECs were incubated with cy5.5 labeled tTF-AS1411, AS1411, tTF or saline, respectively. For V-HUVECs group, flow cytometry analysis suggested a strong fluorescent intensity after tTF-AS1411 treatment, which is comparable to AS1411 treatment and much higher than tTF or saline control (Fig. 2B). In contrast, none of these agents could bind to the control N-HUVECs (Supporting Information Fig. S2). When an anti-nucleolin antibody was utilized to pre-incubate the cells, the binding ability of tTF-AS1411 to V-HUVECs was blocked, indicating the binding is specific for nucelolin expression (Fig. 2B). Confocal microscopy further confirmed a high and specific binding of tTF-AS1411 to V-HUVECs (Fig. 2C, and Supporting Information Fig. S3). Furthermore, cytotoxicity assay showed that tTF-AS1411 and AS1411 treatment exhibited a strong cytotoxicity in the V-HUVECs but not to N-HUVECs (Supporting Information Fig. S4). Taken together, these data demonstrated that tTF-AS1411 conjugate has high specificity for binding to malignant vascular endothelial cells but not normal endothelial cells, subsequently leading to strong cell killing effect.

3.3. *In vivo biodistribution and pharmacokinetics*

To explore the tumor targeting ability of tTF-AS1411 *in vivo,* we intravenously administered the Cy5.5 labeled conjugates into BALB/c nude mice bearing human liver cancer MHCC-97H tumor xenografts, and tissue samples were obtained at different time points. Notably, the tumor had a significantly higher fluorescence intensity as compared with free tTF from 4 h after administration of the same dose of tTF-AS1411 (Fig. 3A, B and S5). Equally important, the conjugation of tTF to AS1411 significantly reduced tTF accumulation at several non-tumor sites in the body, especially the liver and kidney (Supporting Information Fig. 3A and S5). In particular, the half-life of tTF-AS1411 in the mouse plasma was longer than that free tTF, as measured as a function of time post injection (Fig. 3C and D). These results suggested that tTF-AS1411 is likely to preferentially accumulate in solid tumors as compared with free tTF.

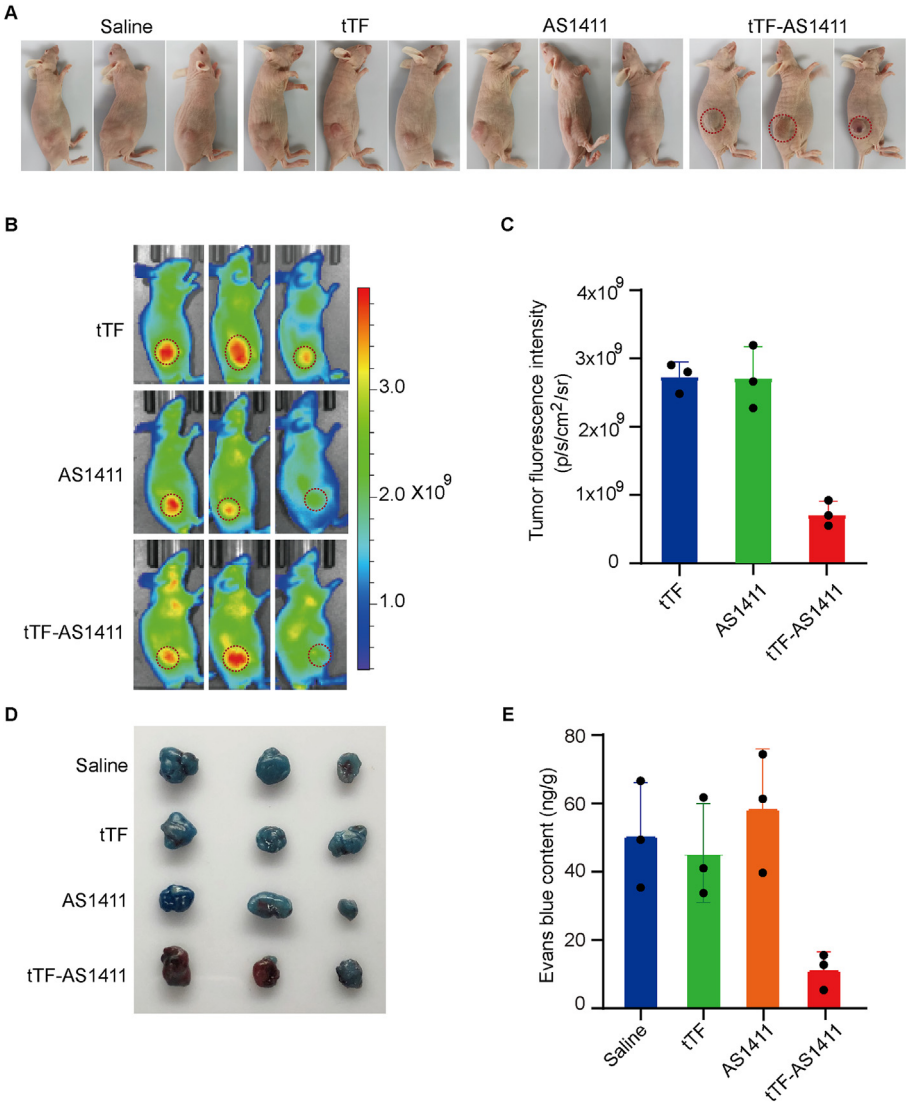

Figure 4 tTF-AS1411 induces intratumoral thrombosis and reduces blood perfusion. (A) The gross appearance of MHCC-97H liver tumors 10 h after the first intravenous administration of tTF-AS1411 or controls into the mice. Significant bruising was observed in the tTF-AS1411 group, indicating blood pooling due to vascular occlusion, $n = 3$. (B) Near infrared reflection (NIR) imaging was performed on MHCC-97H tumor-bearing mice after administering Angio-Sense 680EX imaging agent, with pre-treatment of tTF-AS1411, $n = 3$. (C) Quantitative analysis of the AngioSense 680EX signal intensities in tumors. Error bars represent the mean ± SD, $n = 3$, $^{***}P < 0.01$. (D) Representative images of MHCC-97H liver tumors from mice treated with Evans blue (5%) after pre-treatment with tTF-AS1411 or controls. Evans blue accumulation was significantly decreased in the tTF-AS1411 pre-treated tumors, $n = 3$. (E) Quantification of Evans blue contents in different tumors. Error bars represent the mean ± SD; $^{***}P < 0.001$.

3.4. Reduction of the blood perfusion of tumor tissues by tTF-AS1411 treatment

To evaluate the thrombosis induced ability of tTF-AS1411 *in vivo*, MHCC-97H liver tumor-bearing mice were administered tTF-AS1411 or tTF alone through the tail vein at a dosage of 20 μg tTF/mouse. Ten hours after administration, the tumors from tTF-AS1411 but not saline or tTF-treated mice, displayed obvious bruised and blackened color (Fig. 4A), suggesting the thrombotic formation and vascular occlusion. Hematoxylin and eosin (H&E) staining also showed massive thromboses and visible necrosis only in the tTF-AS1411-treated tumors after three administrations (Supporting Information Fig. S6). Quantitative analysis further revealed more than 80% cellular apoptosis in the tumors (Supporting Information Fig. S7), which was greater by 3 folds compared with the saline or tTF-treated tumors. To explore the effect of tTF-AS1411 induced thrombosis on blood supply of the tumors, we visualized the blood pooling in the tumors using the vascular fluorescent imaging probe AngioSense 680EX that is distributed passively through vascular leaks and remains localized in the tumors with a peak at approximately 24 h. We pre-treated MHCC-97H liver tumor bearing mice with saline or tTF-AS1411 at a dose of 20 μg tTF/mouse. Ten hours later, 2 nmol AngioSense 680EX was administered intravenously into the mice

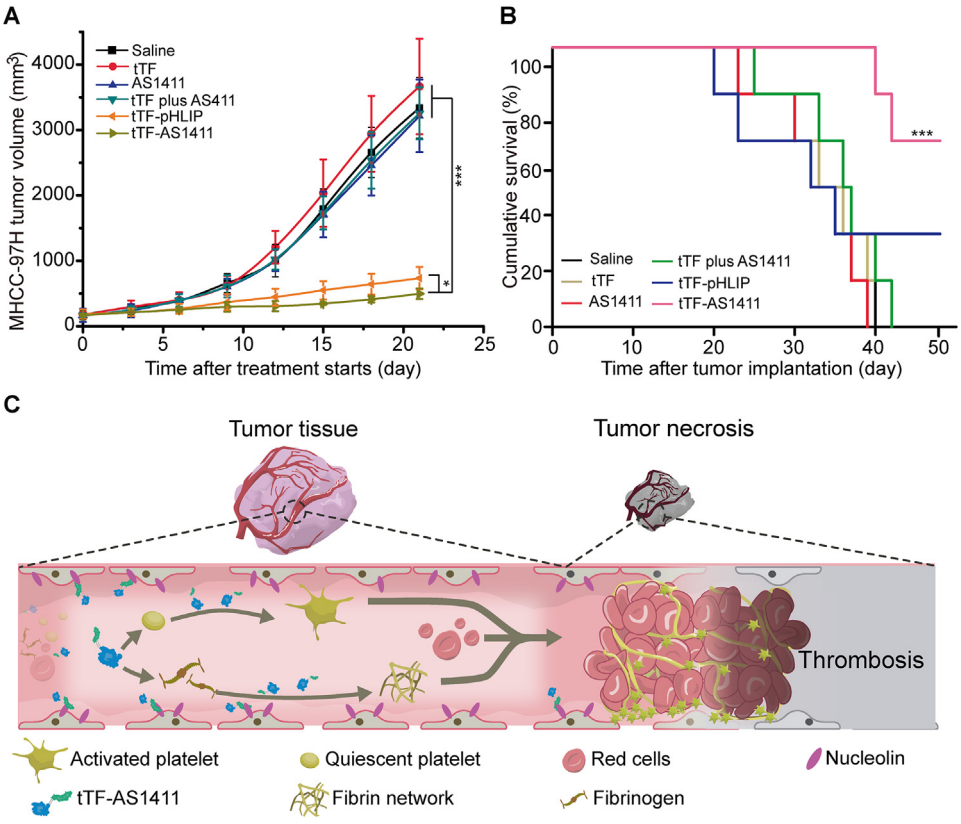

Figure 5 Antitumor activity of tTF-AS1411. (A) tTF-AS1411 significantly inhibited the growth of MHCC-97H liver tumors in mice compared with various controls. Error bars represent the mean ± SD, $n = 6$; *$P < 0.05$, ***$P < 0.001$. (B) Cumulative survival of MHCC-97H tumor-bearing mice. Error bars represent the mean ± SD, $n = 6$; ***$P < 0.001$. (C) Schematic illustration of the hypothesized action of tTF-AS1411 within tumor vessels. Thrombus formation occurs when tTF-AS1411 binds to nucleolin receptors on vascular endothelial surfaces, thus resulting in tumor necrosis and inhibition.

and the *in vivo* optical imaging was taken at 680 nm after another 24 h, recording the fluorescence signal of tumor tissue (Fig. 4B). Pre-treating tumors with tTF-AS1411 dramatically reduced the fluorescent signal of tumors compared with saline group. Further quantitative data revealed an approximate 70% reduction in the signal intensity after tTF-AS1411 treatment (Fig. 4C), indicating a blocked blood perfusion. To confirm these observations, we assessed the intra-tumor delivery efficiency of macromolecular Evans blue after pre-administration of tTF-AS1411. The results suggested that the tumor had a significant two to three folds decrease in Evans blue accumulation 24 h after intravenous administration as compared with saline or free tTF pre-treated tumors (Fig. 4D and E). Thus, tTF-AS1411 treatment is able to substantially reduce the blood perfusion of tumor tissues.

3.5. *Antitumor activity of tTF-AS1411*

tTF-AS1411 conjugates were next evaluated for their anti-tumor activity. Mice with MHCC-97H liver tumors were intravenously treated with tTF-AS1411, free tTF, AS1411, free tTF plus AS1411, tTF-pHLIP (as a positive control) or saline at an interval of six days for a total of three times (Supporting Information Fig. S8A). tTF-pHLIP is a fusion protein that we have described in a previous work[8]. This fusion protein can respond to the acidic environment in the tumor and efficiently induced the thrombotic occlusion of tumor vessels. Nine days later, a significant degradation in tumor volume was observed in both tTF-AS1411 and tTF-pHLIP groups compared with other control groups (Fig. 5A, and Supporting Information Fig. S9), which correlated with the substantial increase in animal survival (Fig. 5B). More than 60% of the mice were still alive on day 45 after cessation of tTF-AS1411 and tTF-pHLIP treatment, respectively; however, none of the mice survived in the other control groups. It should be noted that the inhibitory effect of tTF-AS1411 is greater than tTF-pHLIP which exhibited superior therapeutic effect as a peptide directed vascular occlusion agent in our previous study. Although treatment with AS1411 alone slightly delayed the tumor growth over time compared with saline, no statistically significant differences in tumor volumes were found between these two groups after cessation of treatment. The weak inhibition of AS1411 on tumor growth presumably derives from its slight cell-killing effect under current dosage. We also evaluated the therapeutic efficiency of tTF-AS1411 in B16−F10 melanoma tumor-bearing mice using the same protocol as for the MHCC-97H liver tumors. Similarly, tTF-AS1411 exhibited significant inhibition on tumor growth compared with various control formulations (Figs. S8B and S9). This inhibitory effect dramatically prolonged the animal survival to 50 days in contrast to the 23 days median survival of the saline group (Fig. S8C). Thus, with several dose injections, tTF-AS1411 provides a substantial therapeutic effect by inducing intratumor thrombosis and tumor necrosis (Fig. 5C).

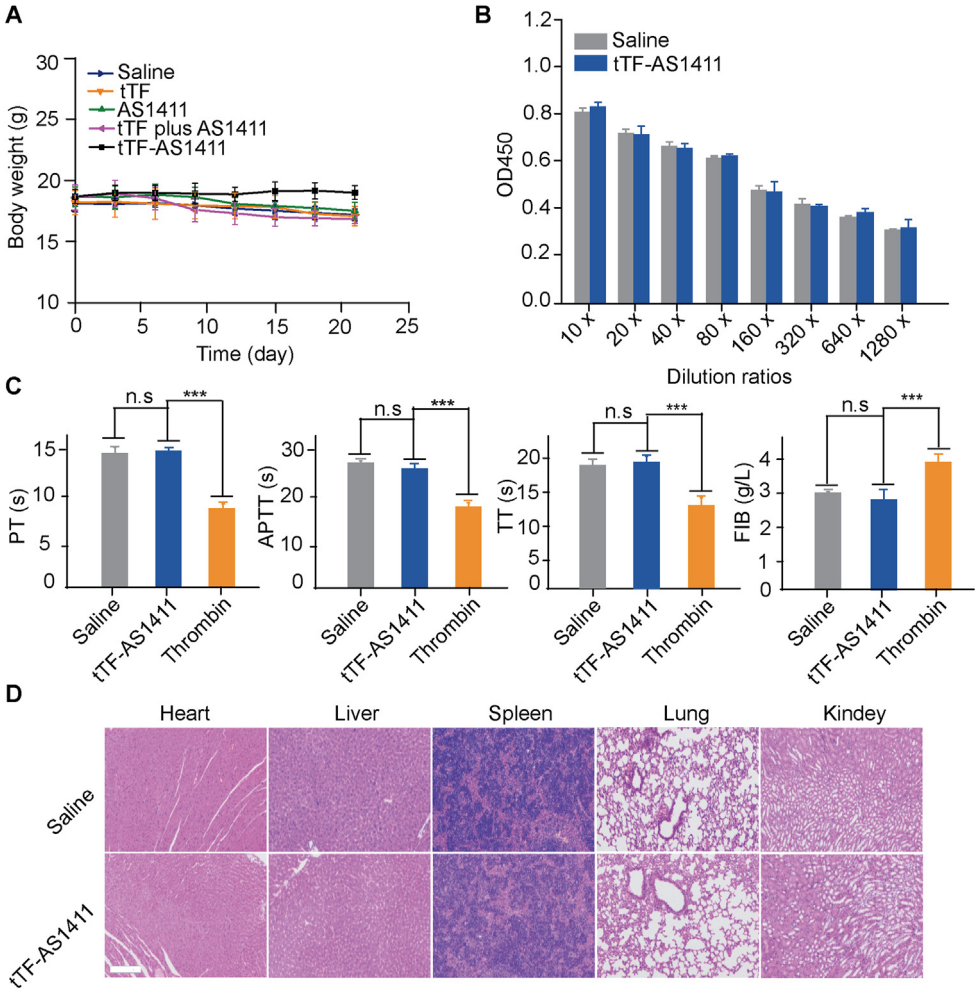

Figure 6 Safety assessment of tTF-AS1411. (A) The body weights of the MHCC-97H liver tumor-bearing mice were recorded every three days during the *in vivo* therapeutic process. Each point of the data indicates the mean ± SD, $n = 6$). (B) Whole blood was collected from MHCC-97H liver tumor-bearing mice. The serum was tested for antibodies against tTF using a standard indirect ELISA experiment. No differences were detected at any of the tested dilutions between the saline and tTF-AS1411 groups. Each bar represents the mean ± SD, $n = 6$). (C) Whole blood was collected from MHCC-97H tumor-bearing mice after saline, tTF-AS1411 or thrombin injections. The coagulation indices, including prothrombin time (PT), activated partial thromboplastin time (APTT), thrombin time (TT) and fibrinogen (FIB) were measured. The data are presented as the mean ± SD, $n = 6$; $^{*}P < 0.05$, $^{**}P < 0.01$, and $^{***}P < 0.001$, ns, not significant. (D) H&E stained microphotographs of major organs. Sections of the heart, liver, spleen, lung and kidney were stained with H&E. No thrombosis was apparent in any of the organs in the tTF-AS1411 treated MHCC-97H tumor-bearing mice. Scale bar = 100 μm.

3.6. Safety evaluation of tTF-AS1411

We finally investigated the safety of tTF-AS1411 *in vivo*. Throughout the therapeutic experiments, tTF-AS1411 treatment neither significantly affected the animals' body weights (Fig. 6A) nor caused any morbidity or mortality, suggesting that tTF-AS1411 is of no or low toxicity to the mice. The results of ELISA experiments suggested that no differences in antibody titer were detected in the serum from the mice treated with tTF-AS1411 and saline (Fig. 6B), indicating the immune inert of tTF-AS1411. To investigate whether tTF-AS1411 treatment activates the coagulation system in the body, we examined coagulation related indicators, including fibrinogen (FIB), prothrombin time (PT), thrombin time (TT) and activated partial thromboplastin time (APTT), in the plasma from normal BALB/c nude mice 24 h after tTF-AS1411 administration. No apparent differences were observed in any indicator between tTF-AS1411 and saline-treated groups. By contrast, a certain amount of thrombin treatment (positive control) resulted in a significant change in all indicators (Fig. 6C). In addition, H&E staining demonstrated no observable thromboses in major organs (heart, liver, spleen, lung and kidney) of the tTF-AS1411 treated mice (Fig. 6D), indicating the high selectivity of tTF-AS1411 for tumor tissues.

4 Conclusions

The molecular engineered tTF-AS1411 conjugate described here present three important points of novelty: (1) it not only enhanced the targeting ability of tTF to tumor tissues, but also realized the combined therapy of vascular infarction with the direct cell killing

effect of aptamer in one molecular structure manner, achieving maximal therapeutic effect; (2) it was easy to prepare in a simple two-step synthesis with high yield, purity and low costs; (3) it degraded into non-toxic components to enable clearance from the body, as this conjugate consisted of polypeptides and DNA sequences. We believe that this combination of advantages makes the tTF-AS1411 conjugate uniquely attractive as a new tumor vascular occlusion agent with promise for clinical application for cancer therapy.

Acknowledgments

This work was supported by grants from the National R&D Program of China (2018YFE0205300, 2018YFA0208900), the National Natural Science Foundation of China (81871489, 91859118, 31730032, 31700870, 31470969, 31661130152), the National Distinguished Young Scientist program (31325010, China), the K.C. Wong Education Foundation (GJTD-2018-03, China), and the Beijing Municipal Natural Science Foundation (7182126, China).

Author contributions

Suping Li, Guangjun Nie and Jingyan Wei supervised the work. Bozhao Li performed all experiments. Bozhao Li, Suping Li and Guangjun Nie wrote the manuscript. Yinlong Zhang, Chunzhi Di, WeiSun Leong, Lele Li provided the technical support. Feilong Qi, Zefang Lu helped with manuscript revision and data collection.

Conflicts of interest

The authors declare no competing financial interest.

Appendix A. Supporting information

Supporting data to this article can be found online at https://doi.org/10.1016/j.apsb.2020.11.014.

References

1. Folkman J. Angiogenesis in cancer, vascular, rheumatoid and other disease. *Nat Med* 1995;**1**:27−31.
2. Vikash P, Rakesh K. Strategies for advancing cancer nanomedicine. *Nat Mater* 2013;**12**:958−62.
3. Kessler T, Schwoppe C, Liersch R, Schliemann C, Hintelmann H, Bieker R, et al. Generation of fusion proteins for selective occlusion of tumor vessels. *Curr Drug Discov Technol* 2008;**5**:1−8.
4. Li SP, Zhang YL, Ho SH, Li BZ, Wang MF, Deng XW, et al. Combination of tumour-infarction therapy and chemotherapy *via* the co-delivery of doxorubicin and thrombin encapsulated in tumour-targeted nanoparticles. *Nat Biomed Eng* 2020;**4**:732−42.
5. Hu PS, Yan JH, Sharifi J, Bai T, Khawli LA, Epstein AL. Comparison of three different targeted tissue factor fusion proteins for inducing tumor vessel thrombosis. *Cancer Res* 2003;**63**:5046−53.
6. Huang XM, Molema G, King S, Watkins L, Edgington TS, Thorpe PE. Tumor infarction in mice by antibody-directed targeting of tissue factor to tumor vasculature. *Science* 1997;**275**:547−50.
7. Nilsson F, Kosmehl H, Zardi L, Neri D. Targeted delivery of tissue factor to the ED-B domain of fibronectin, a marker of angiogenesis, mediates the infarction of solid tumors in mice. *Cancer Res* 2001;**61**:711−6.
8. Li SP, Tian YH, Zhao Y, Zhang YL, Su SS, Wang J, et al. pHLIP-mediated targeting of truncated tissue factor to tumor vessels causes vascular occlusion and impairs tumor growth. *Oncotarget* 2015;**6**:23523−32.
9. Bieker R, Kessler T, Schwoppe C, Padro T, Persigehl T, Bremer C, et al. Infarction of tumor vessels by NGR-peptide-directed targeting of tissue factor: experimental results and first-in-man experience. *Blood* 2009;**113**:5019−27.
10. Dorfleutner A, Ruf W. Regulation of tissue factor cytoplasmic domain phosphorylation by palmitoylation. *Blood* 2003;**102**:3998−4005.
11. Shi QW, Zhang YL, Liu SL, Liu GN, Xu JC, Zhao X, et al. Specific tissue factor delivery using a tumor-homing peptide for inducing tumor infarction. *Biochem Pharmacol* 2018;**156**:501−10.
12. Ruf W, Edgington TS. Structural biology of tissue factor, the initiator of thrombogenesis *in vivo*. *FASEB J* 1994;**8**:385−90.
13. Ruf W, Rehemtulla A, Morrissey JH, Edgington TS. Phospholipid-independent and -dependent interactions required for tissue factor receptor and cofactor function. *J Biol Chem* 1991;**266**:2158−66.
14. Liu SL, Zhang YL, Zhao X, Wang J, Di CZ, Zhao Y, et al. Tumor-specific silencing of tissue factor suppresses metastasis and prevents cancer-associated hypercoagulability. *Nano Lett* 2019;**19**:4721−30.
15. Huang X, Ding WQ, Vaught JL, Wolf RF, Morrissey JH, Harrison RG, et al. A soluble tissue factor-annexin V chimeric protein has both procoagulant and anticoagulant properties. *Blood* 2006;**107**:980−6.
16. Butenas S, Orfeo T, Mann KG. Tissue factor in coagulation which? where? when. *Arterioscler Thromb Vasc Biol* 2009;**29**:1989−96.
17. Butenas S, Mann KG. Active tissue factor in blood. *Nat Med* 2004;**10**:1155−6.
18. Ding YP, Li SP, Nie GJ. Nanotechnological strategies for therapeutic targeting of tumor vasculature. *Nanomedicine* 2013;**8**:1209−22.
19. Bogdanov VY, Versteeg HH. "Soluble tissue factor" in the 21st century: definitions, biochemistry, and pathophysiological role in thrombus formation. *Semin Thromb Hemost* 2015;**41**:700−7.
20. Eisenreich A, Bolbrinker J, Leppert U. Tissue factor: a conventional or alternative target in cancer therapy. *Clin Chem* 2016;**62**:563−70.
21. Rosenberg JE, Bambury RM, Van Allen EM, Drabkin HA, Larajr PN, Harzstark AL, et al. A phase II trial of AS1411 (a novel nucleolin-targeted DNA aptamer) in metastatic renal cell carcinoma. *Invest N Drugs* 2014;**32**:178−87.
22. Bates PJ, Laber DA, Miller DM, Thomas SD, Trent JO. Discovery and development of the G-rich oligonucleotide AS1411 as a novel treatment for cancer. *Exp Mol Pathol* 2009;**86**:151−64.
23. Li LY, Hou JJ, Liu XJ, Guo YJ, Wu Y, Zhang LH, et al. Nucleolin-targeting liposomes guided by aptamer AS1411 for the delivery of siRNA for the treatment of malignant melanomas. *Biomaterials* 2014;**35**:3840−50.
24. Soundararajan S, Wang L, Sridharan V, Chen WW, Courtenay-Luck N, Jones D, et al. Plasma membrane nucleolin is a receptor for the anticancer aptamer AS1411 in MV4-11 leukemia cells. *Mol Pharmacol* 2009;**76**:984−91.
25. Ireson CR, Kelland LR. Discovery and development of anticancer aptamers. *Mol Canc Therapeut* 2006;**5**:2957−62.
26. Soundararajan S, Chen WW, Spicer EK, Courtenay-Luck N, Fernandes DJ. The nucleolin targeting aptamer AS1411 destabilizes Bcl-2 messenger RNA in human breast cancer cells. *Cancer Res* 2008;**68**:2358−65.
27. Reyes-Reyes EM, Teng Y, Bates PJ. A new paradigm for aptamer therapeutic AS1411 action: uptake by macropinocytosis and its stimulation by a nucleolin-dependent mechanism. *Cancer Res* 2010;**70**:8617−29.
28. Zhu HJ, Li J, Zhang XB, Ye M, Tan WH. Nucleic acid aptamer-mediated drug delivery for targeted cancer therapy. *ChemMedChem* 2015;**10**:39−45.
29. Keefe AD, Pai S, Ellington A. Aptamers as therapeutics. *Nat Rev Drug Discov* 2010;**9**:537−50.

30. Zhou JH, Rossi J. Aptamers as targeted therapeutics: current potential and challenges. *Nat Rev Drug Discov* 2017;**16**:181−202.
31. He JX, Peng TH, Peng YB, Ai LL, Deng ZY, Wang XQ, et al. Molecularly engineering triptolide with aptamers for high specificity and cytotoxicity for triple-negative breast cancer. *J Am Chem Soc* 2020;**142**:2699−703.
32. Yang QX, Deng ZY, Wang D, He JX, Zhang DL, Tan Y, et al. Conjugating aptamer and mitomycin C with reductant-responsive linker leading to synergistically enhanced anticancer effect. *J Am Chem Soc* 2020;**142**:2532−40.
33. Li SP, Jiang Q, Liu SL, Zhang YL, Tian YH, Song C, et al. A DNA nanorobot functions as a cancer therapeutic in response to a molecular trigger *in vivo*. *Nat Biotechnol* 2018;**36**:258−64.
34. Teng IT, Li XW, Yadikar HA, Yang ZH, Li L, Lyu YF, et al. Identification and characterization of DNA aptamers specific for phosphorylation epitopes of Tau protein. *J Am Chem Soc* 2018;**140**:14314−23.
35. Joyce JA, Laakkonen P, Bernasconi M, Bergers G, Ruoslahti E, Hanahan D. Stage-specific vascular markers revealed by phage display in a mouse model of pancreatic islet tumorigenesis. *Cancer Cell* 2003; **4**:393−403.